EB2020-FBR-027

A comparison of methods for characterizing brake pad surfaces

Fabian Limmer* [1], Andreas Paulus[2], David Barton [1], Peter Brooks [1], Anne Neville [1], Shahriar Kosarieh [1]

[1]University of Leeds, School of Mechanical Engineering, Woodhouse Lane, Leeds LS29JT, United Kingdom (E-mail: mnfli@leeds.ac.uk)

[2] TMD Friction Services GmbH, Schlebuscher Straße 99, 51381 Leverkusen, Germany

https://doi.org/10.46720/EB2020-FRB-027

ABSTRACT: The brake industry is currently driven towards lighter, corrosion resistant and more eco-friendly brake systems in order to meet the current health and environmental demands and megatrends of electrification and autonomous driving. While trying to meet these new demands, there is no room for compromising the brake systems friction and wear performance. Understanding the friction interface of the brake system is therefore key to being able to meet these often-contradicting demands. The contact situation in the friction interface is generally described by a friction layer that is formed during the braking process. The friction layer makes up the real contact area between the static brake pad and the rotating brake disc. It is only a fraction of the size of the apparent pad area and is present in the form of so-called contact plateaux. This study compares the method of image segmentation that utilizes a light microscope to capture the contact plateaux of a brake pad surface with a different method that uses a focused ion beam for the detection of the contact plateaux.

KEY WORDS: Brake pad, real contact area, contact plateaux, surface topography

1. Introduction

The frictional and wear performance of brake systems has long been linked to the presence of a so called third body layer (tbl). This third body layer separates the two first bodies (brake disc and brake pad) during the braking process and ensures velocity accommodation, load bearing and protection of the first bodies against excessive wear [1]. Originating mostly through wear resistant components of the brake pad (primary contact plateaux), the third body consists mainly of compacted wear debris from the first bodies (secondary plateaux). Although described as a layer, the geometrical presence of the third body on the brake pad surface is in the form of a discontinuous patch-like structure often referred to as a contact plateau. During braking, the contact plateaux undergo continuous processes of formation, growth and destruction. The equilibrium state of these processes determines the real contact area that transmits the friction force during braking and therefore the tbl is one important factor that determines the coefficient of friction [2].

Since the real contact area is not easily accessible during the braking process (in-situ), many past investigations have focused on developing methods for characterizing the brake pad surface after or in between braking applications (ex-situ) [3-6].

This work aims to compare two very different methods that deliver similar outputs. One method relies on the reflection of light whereas the other method relies on the emission of electrons. The outputs of both methods are high contrast images where the contact plateaux are shown very brightly compared to the areas that haven't been in contact during braking.

2. Materials & Methods

2.1. Samples

The friction material was copper free and can be classified as Low Met (Low metallic content) or Low Steel, meaning it will have a steel content of roughly 20 % by weight [7]. The brake pad sample had a rectangular shape with the dimensions 30 x 10 x 10 mm. The brake disc was made from grey cast iron (EN GJL 250) and had a diameter of 100 mm and a solid thickness of 10 mm. The surface of the disc was prepared using 320 grit sandpaper prior to testing.

2.2. Braking test

A Bruker UMT TriboLab was used to perform the tests on a small-scale basis. The temperature was measured during the test on the surface of the brake disc next to the braking track with a rubbing thermocouple. First, the samples were subjected to a running-in procedure consisting of permanent braking for one hour under a nominal surface pressure of 0.125 MPa and a sliding speed of 6 m/s. Afterwards, 200 drag brake applications were performed at a nominal pressure of 0.5 MPa and a sliding speed of 9.2 m/s. Each application had a duration of 15 seconds with 10 seconds in between each application. The brake disc temperature rose from 40 °C up to 235 °C during the test. After the test, the brake pad was placed on a SEM specimen stub and the sides of the brake pad were additionally covered with a carbon paint. The rubbing surface of the brake pad was not further treated after testing (not blown with air, etc.).

2.3. Imaging devices

A ThermoFischer Scientific Helios G4 CX DualBeam microscope was used for the Scanning Ion Microscopy (SIM) and the Energy-Dispersive X-ray Spectroscopy (EDS). The secondary electrons were detected with an Everhart-Thornley Detector (ETD). The Light Microscope (LM) images were taken using a Keyence VHX-6000 digital microscope. Surface height measurements were performed using a Bruker NPFLEX white light interferometer (WLI). The settings are shown in Table 1.

Table 1 Imaging device settings

	Voltage	Current	Magnification
SIM	30kV	24pA	700x
EDS	15kV	6.4nA	500x
LM	-	-	50x
WLI	-	-	20x

Image stitching was used with all the imaging devices in order to obtain a large enough surface area of the brake pad. Starting with the light microscope, the complete 10x30mm surface of the brake pad was captured (Figure 1).

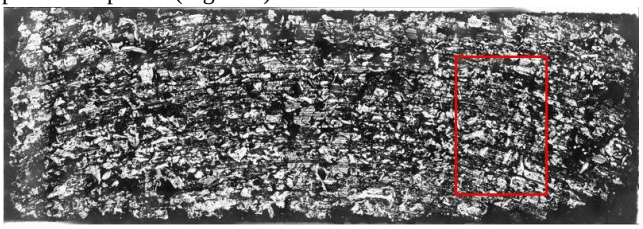

Figure 1 Friction material surface (10×30mm) captured with LM

An area of 4.24×6.22mm was chosen for further evaluation (red frame in Figure 1) and the image was cropped to the corresponding size. The same brake pad area was captured with the dual beam microscope and the images were then aligned and cropped to the same dimensions using the Freeware ImageJ together with the DS4H image alignment plugin [8]. Figure 2 shows the LM image (left) next to the SIM image of the same 4.24×6.22mm area (right).

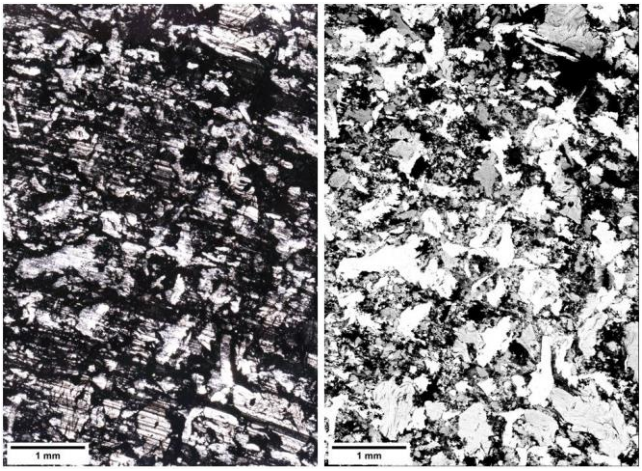

Figure 2 Friction material surface (4.24×6.22mm) captured with LM (left) and SIM (right)

Both images in Figure 2 show the contact plateaux in bright colour whereas the non-contacting areas appear dark. The two selected techniques rely on completely different measurement principles when generating the high contrast images. Scanning ion microscopy was first used for this application by Österle [5]. He found the main mechanism behind the contrast images to be exoelectron emission (EE). EE occurs for example when materials are being highly stressed. The plastic deformation and adhesion processes as well as the chemical reactions (formation of oxide layers) taking place during braking cause the contacting areas to emit a higher number of electrons after being excited by the ion beam [9,10].

The high contrast of the light microscope images is generated based on the idea that the contact plateaux are all roughly on the same height (focal plane) and are much smoother than non-contacting areas and therefore will reflect more light. This method has more recently been applied by the group of Neis [6], who also used Otsu's thresholding method [11] for the image binarization.

2.4 Image processing

Further processing was conducted using a purpose-written MATLAB script. In a first step, the images were converted into grey scale images and then binarized using Otsu's method [11]. Contact plateaux have been reported to be present in the size range of 50 – 500 µm [12]. In this study, contact plateaux smaller than 50 µm are regarded as being in a "birth state" where they are not significantly contributing to the friction force. Using the µm/pixel ratio known from the horizontal field width of the SIM images, all contact plateaux (white areas) smaller than 1900 µm² were filtered from the images. This will also ensure that any numerical noise is removed from the images. Figure 3 shows the LM image (left) next to the SIM image (right) after processing through the MATLAB script.

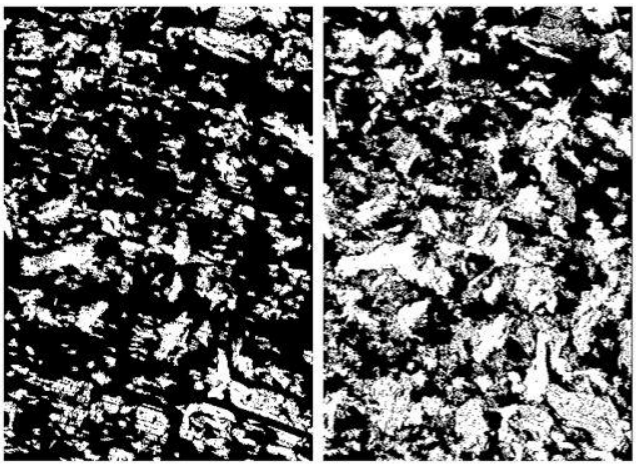

Figure 3 Processed images (4.24×6.22mm) from LM (left) and from SIM (right)

3. Results

The images were compared by quantitative and qualitative means. Popular quantitative parameters when analysing brake pad surfaces

are the percentage of real contact area in relation to the apparent contact area (number of white pixels compared to the overall pixel amount), the average area of the contact plateaux and the contact plateau density (number of plateaux on captured surface). Table 2 shows the results of the quantitative analysis of the images shown in Figure 3.

Table 2 Quantitative friction material surface parameters

	LM	SIM
Real contact area [%]	26	43
Avg. contact plateau area [µm²]	15931	118370
Contact plateau density [n/mm²]	16	5

All surface parameters in Table 2 show a great difference between the LM and SIM results. Especially the average contact plateau area is very large for the SIM image. The reason for this is because many of the contact plateaux in the SIM image are linked together. The software then recognizes the linked plateau as one plateau only. The contact plateau density is therefore much lower for the SIM image than for the LM image.

For the qualitative comparison, the processed LM image was subtracted from the processed SIM image to reveal the difference in the two images (Figure 4).

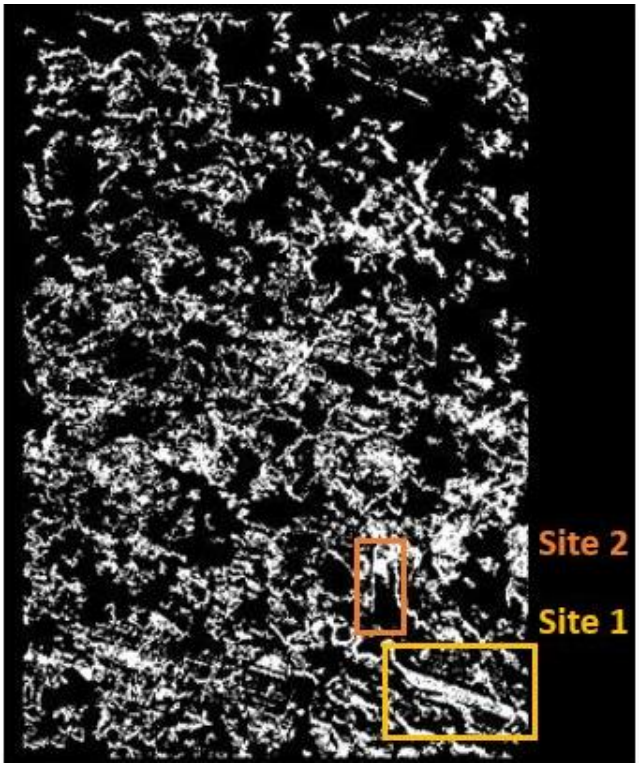

Figure 4 Difference of the edited LM and SIM image for the 4.24×6.22mm section

The large part of the contact plateaux is captured by both methods. Figure 4 reveals that the biggest difference in the two images lies in the grooves on the contact plateaux. The grooves on the contact plateaux are created through interactions with the brake disc surface structure. During braking, the disc will abrade a negative image of its current surface structure into the contact plateaux. With the grooves being deeper than the rest of the contact plateau surface and the surfaces of the grooves not being perpendicular to the microscope objective, the grooves appear dark in the LM images. A SEM close-up on one of the contact plateaux that shows such a difference is shown in Figure 5.

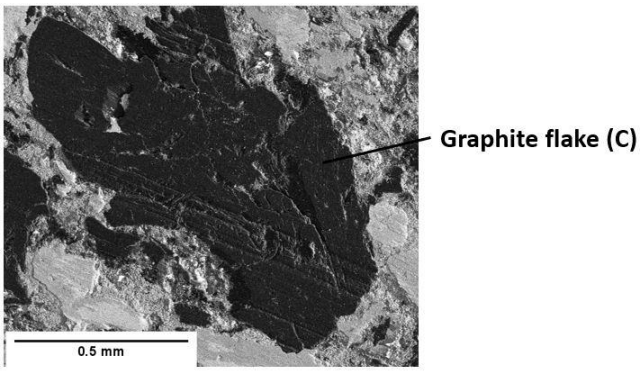

Figure 5 SEM image of a contact plateau (site 1)

From the combined information of the SEM image shown in Figure 5 together with the EDS data, it can be concluded that the contact plateau consists of a graphite flake.

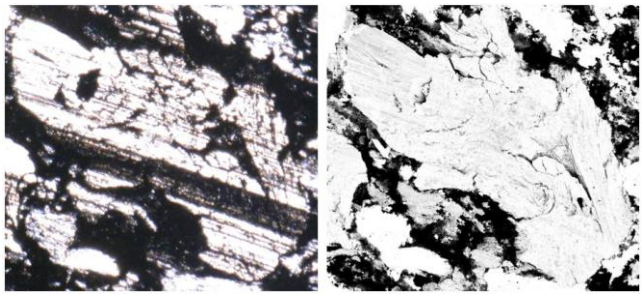

Figure 6 LM image (left) and SIM image (right) of the contact plateau (site 1)

The SIM image (Figure 6 right) shows the graphite flake in a uniform brightness. Since even very thin third body layers would show in SIM imaging because of the low interaction depth of the ions with the sample, it can be concluded that the graphite flake is not covered by a third body layer. The LM image on the left of Figure 6 shows the same graphite flake with a big wear scar across its centre that appears dark in this image whereas the wear scar is not visible in the SIM image. This is also one of the reasons for the higher contact plateau density found for the LM image (Table 2). The software recognizes the contact plateau that is separated through the wear scar as two smaller plateaux.

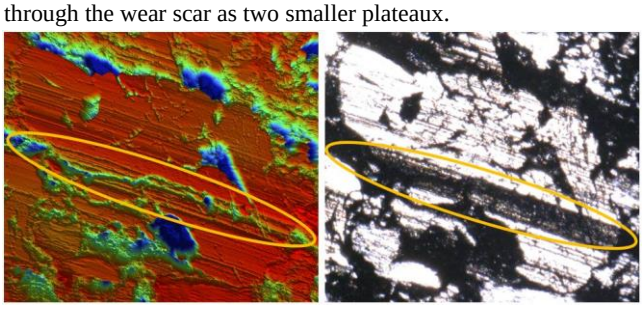

Figure 7 WLI height profile (left) and LM image (right) showing the wear scar on the contact plateau (site 1)

Using white light interferometry, a height profile of the contact plateau at site 1 was taken (Figure 7 left) showing the wear scar across the graphite flake. It is worth mentioning that the captured area proved to be level enough so that no tilt correction was needed.

Another reason for the different output of the two methods lies in the higher surface roughness of the contact plateaux. Although the contact plateaux are generally smoother than the rest of the brake pad surface, some parts of the plateaux surfaces are rough enough to scatter the light at a greater angle so that this light won't be reflected into the objective of the microscope.

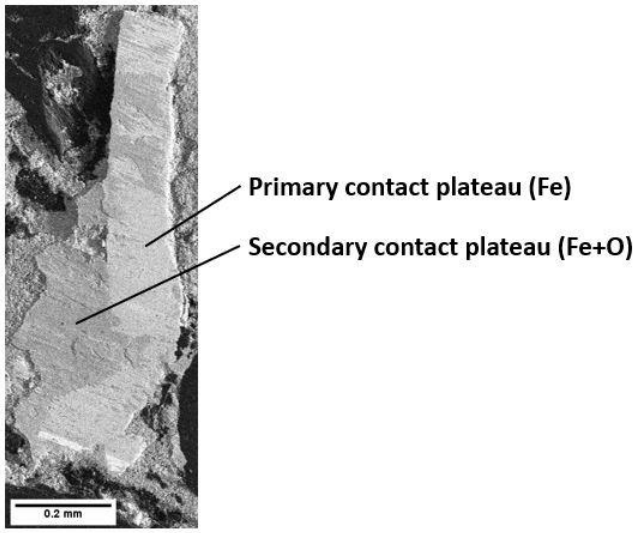

Figure 8 SEM image of a contact plateau at site 2

A SEM closeup on a second site of one of the contact plateaux (Figure 8) shows, that it consists of a metal fibre (primary contact plateau) together with third body material partly on top of the fibre and partly piled up in front of it (secondary contact plateau). The elemental information shown in Figure 8 was taken from the EDS map.

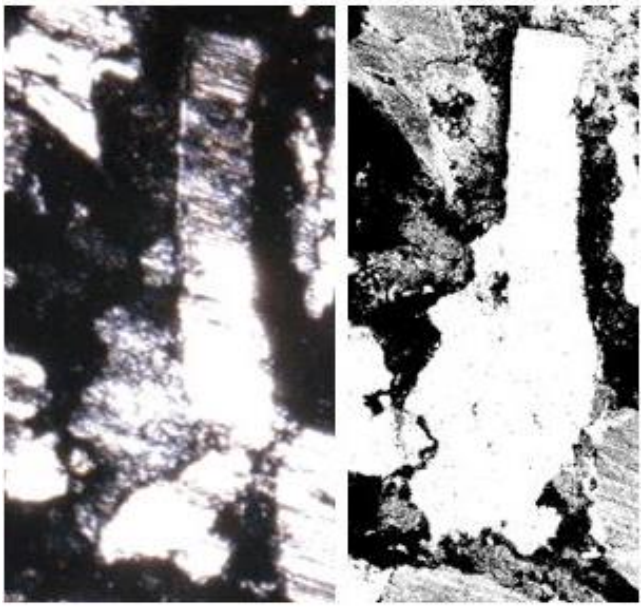

Figure 9 LM image (left) and SIM image (right) of the contact plateau (site 2)

The SIM image (Figure 9 right) of the same contact plateau shown in Figure 8 shows the metal fibre in a uniform brightness together with the third body. The LM image (Figure 9 left) shows the top part of the metal fibre darker than the SIM image and there is a visible border to the secondary contact plateau as well. With the SIM image showing the metal fibre and the third body at a uniform brightness, it can be concluded that both parts participated in load carrying and friction generation.

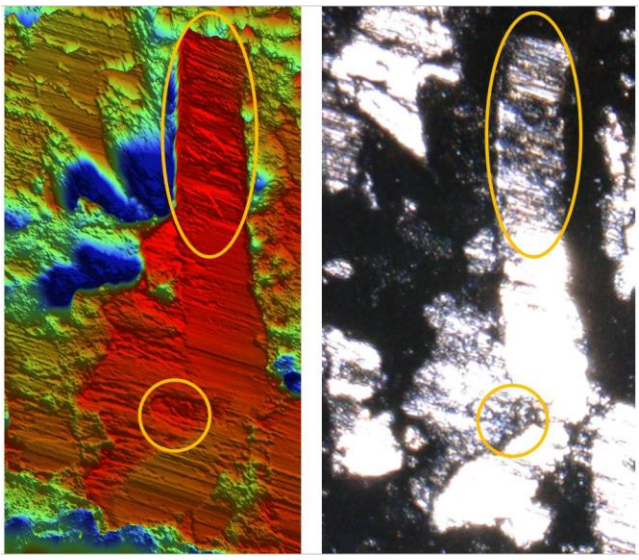

Figure 10 WLI height profile (left) and LM image (right) showing the rougher areas of the contact plateau (site 2)

The height profile (Figure 10 left) shows that those areas that are not identified as contact plateaux in the LM image are areas of higher roughness.

The Dual Beam microscope allowed scanning the sample first with the ion beam and then with the electron beam to obtain the elemental maps without having to move the sample to another microscope. In order to obtain elemental information of the contact plateaux, the binarized SIM image (Figure 3 right) was inverted to show the contact plateaux in black and the non-contacting areas in white. The inverted image was then subtracted from the EDS layered image (of the five most common elements), taking away the colour of the non-contacting areas. The modified EDS layered image now only shows elemental information of the areas that were identified as contact plateaux through the SIM method (Figure 11).

Through colour thresholding using ImageJ, the proportions of the different elements were extracted (Table 3):

Table 3 Proportion of the elements in the contact area

	%
Carbon (C)	33
Iron (Fe) + Oxygen (O)	46
Silicon (Si) + Oxygen (O)	6
Aluminium (Al) + Oxygen (O)	15

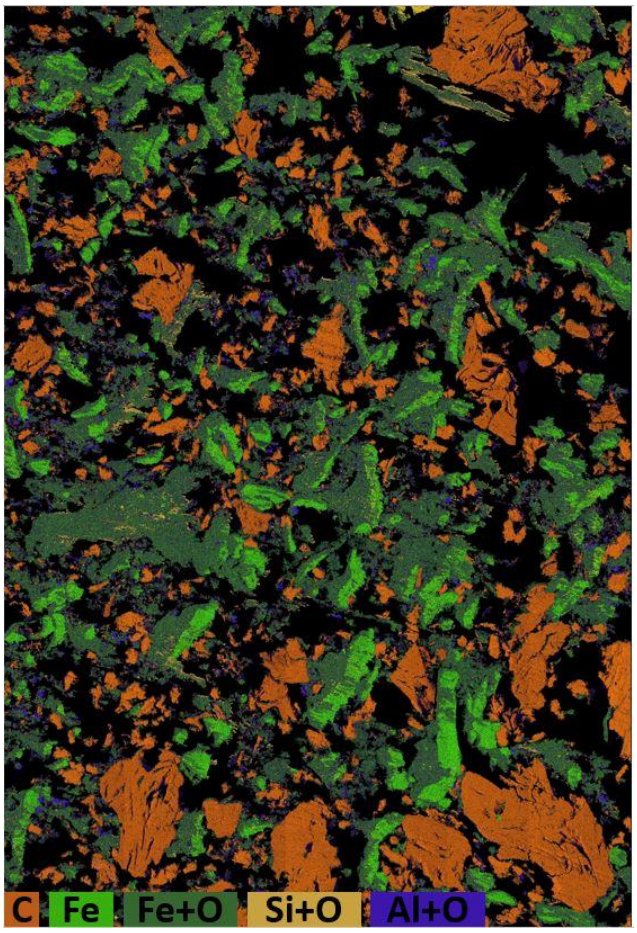

Figure 11 Combined image from the SIM image and EDS map showing the elemental information of the contact plateaux

4. Discussion and Conclusion

The investigations show, that SIM imaging will give a more reliable output when looking at the quantitative parameters such as the real contact area. It is questionable however, how far the average contact plateau area and the contact plateau density can be linked to tribological parameters such as the friction coefficient because most of the contact plateaux are already linked together at the relatively low surface pressures used in this study (0.5MPa). LM imaging on the other hand has great advantages in terms of ease of use, imaging time, cost of operation and capturable size of surface area.

The following conclusions can be drawn from the results:

- SIM and LM both deliver high contrast images showing the contact plateaux on the friction material surface.
- The higher contact area obtained by SIM is largely because the contact plateaux have grooves from the brake disc surface on them that appear dark in the LM images.
- The dark grooves in the LM images sometimes separate a contact plateau, causing it to be detected as two contact plateaux by the software and therefore leading to a lower average contact plateau area and a higher contact plateau density.
- Both methods identify graphite flakes, metal fibres and the third body layer as contact plateaux.

The next steps will be to make some adjustments and corrections to the image processing method in order to be able to use the LM images for quantitative evaluation of the friction material surfaces. Future work will then focus on using the developed technique to study different tribosystems of varied brake pad and disc materials.

References

[1] A.L. Cristol-Bulthé, Y. Desplanques, G. Degallaix. Coupling between friction physical mechanisms and transient thermal phenomena involved in pad-disc contact during railway braking. Wear 263 (7) 2007 1230–1242. https://doi.org/10.1016/j.wear.2006.12.052

[2]G P. Ostermeyer, M. Müller. New insights into the tribology of brake systems. Proceedings of the IMechE, Part D: Journal of Automobile Engineering 222 (7) 2008 1167-1200. https://doi.org/10.1243/09544070JAUTO595

[3] M. Eriksson, F. Bergman, S. Jacobson. Surface characterization of brake pads after running under silent and squealing conditions. Wear 232 (2) 1999 163-167. https://doi.org/10.1016/S0043-1648(99)00141-6

[4] D. Bettge, J. Starcevic. Quantitative description of wear surfaces of disc brakes using interference microscopy. Wear 248 (1-2) 2001 121-127. https://doi.org/10.1016/S0043-1648(00)00551-2

[5] W. Österle, D. Bettge. A comparison of Methods for Characterizing Brake Lining Surfaces. Practical Metallography 41 (10) 2004 494-505. https://doi.org/10.1016/S0043-1648(03)00235-7

[6] P. D. Neis, N. F. Ferreira, J. Sukuraman, P. D. Baets, M. Andró, L. T. Matozo, D. Masotti. Characterization of surface morphology and its correlation with friction performance of brake pads. Sustainable Construction & Design 6 (1) 2015. https://doi.org/10.21825/scad.v6i1.1136

[7] B. Breuer, K. H. Bill. Bremsenhandbuch: Grundlagen, Komponenten, Systeme, Fahrdynamik. Wiesbaden: Springer Vieweg 2017. https://doi.org/10.1007/978-3-658-15489-9

[8] J. Bulgarelli, M. Tazzari, A. M. Granato, L. Ridolfi, S. Maiocchi, F. De Rosa, M. Petrini, E. Pancisi, G. Gentili, B. Vergani, F. Piccinini, A. Carbonaro, B. E. Leone, G. Foschi, V. Ancarani, M. Framarini, M. Guidoboni. Dendritic cell vaccination in metastatic melanoma turns “non-T cell inflamed” into “T-cell inflamed” tumors. Front. Immunol. 10 2352 2019. https://doi.org/10.3389/fimmu.2019.02353

[9]W. Österle, I. Urban. Third body formation on brake pads and rotors. Tribology International 39 (5) 2006 401-408. https://doi.org/10.1016/j.triboint.2005.04.021
[10]L. Oster, V. Yaskolko, J. Haddad. Classification of Exoelectron Emission Mechanisms. Physica Status Solidi 174 (2) 1999 431-439. https://doi.org/10.1002/(SICI)1521-396X(199908)174:2<431::AID-PSSA431>3.0.CO;2-Z
[11]N. Otsu. A Threshold Selection Method from Gray-Level Histograms. IEEE Transactions on Systems, Man, and Cybernetics 9 (1) 1979 62-66. https://doi.org/10.1109/TSMC.1979.4310076
[12]M. Eriksson, S. Jacobson. Tribological surfaces of organic brake pads. Tribology International 33 (12) 2000 817-827. https://doi.org/10.1016/S0301-679X(00)00127-4

Acknowledgement

This work has been funded by the Engineering and Physical Sciences Research Council (EPSRC) Grant no.: EPL01629X1 and TMD Friction Services GmbH.